Colloid and Polymer Science
https://doi.org/10.1007/s00396-019-04573-8

ORIGINAL CONTRIBUTION

Physical principles of the formation of a nanoparticle electric double layer in metal hydrosols

A. P. Gavrilyuk[1,2] · I. L. Isaev[1] · V. S. Gerasimov[1,2] · S. V. Karpov[2,3,4]

Received: 12 July 2019 / Revised: 25 September 2019 / Accepted: 25 September 2019

Abstract

The Brownian dynamics method is employed to study the formation of an electrical double layer (EDL) on the metal nanoparticle (NP) surface in hydrosols during adsorption of electrolyte ions from the interparticle medium. Also studied is the charge accumulation by NPs in the Stern layer. To simulate the process of the formation of EDL, we took into account the effect of image forces and specific adsorption, dissipative and random forces, and the degree of hydration of adsorbed ions on the EDL structure. The employed model makes it possible to determine the charge of NPs and the structure of EDL. For the first time, the charge of both the diffuse part of EDL and the dense Stern layer has been determined. A decrease in the electrolyte concentration (below $c < 0.1$ mol/l) has been found to result in dramatic changes in the formation of the Stern layer.

Keywords Nanoparticle · Adsorption layer · Elastic deformation · Coagulation kinetics · Elasticity modulus

Introduction

The formation of an electric double layer near the surface of colloidal particles is one of the fundamental processes causing a number of non-trivial properties of colloidal systems and their stability.

Synthesis of functional materials containing metallic nanoparticles by reducing metals from their salt solutions in electrolyte media is accompanied by the formation of EDL around the particles and provides aggregative stability of colloidal solutions when attractive van der Waals forces that cause aggregation are counterbalanced by repulsive electrostatic forces produced by overlapping of EDLs [1] of the contacting particles.

Classical theories of EDL formation around NP from electrolytes [2] and the degree of their adequacy are directly related to the accuracy of description of interparticle interactions in colloids. The accuracy of such models determines their predictive capabilities to describe the coagulation kinetics of electrostatically stabilized colloids under specific conditions. Considering the importance of fabricating fundamentally new types of nanoscale elements of nanophotonics with desired properties or nanosensors composed of colloidal NPs, the development of models of pair interparticle interactions is of special attention [3–5].

Understanding the EDL formation mechanisms is of fundamental importance in various areas of science and industrial applications, for example, in ink production and water purification. It also plays a crucial role in widely used technologies such as the metal corrosion control, energy storage, and in a broad range of engineering applications.

Another use of EDL formation on the surface of an electrode is in electric field driven separation processes. In nanochannels and porous media, the formation of EDLs effectively traps ions on the surface. The formation and structure of EDLs in a biological system can determine the behavior of the cell membrane processes [6].

Basically, the description of EDL is based on the approximation of continuous charge distribution. In this case, the finite size of ions is partially taken into account by introducing the Stern layer [2]. The methods of molecular

✉ A. P. Gavrilyuk
glyukonat@icm.krasn.ru

1 Institute of Computational Modeling SB RAS, 660036, Krasnoyarsk, Russia

2 Siberian Federal University, 660041, Krasnoyarsk, Russia

3 L. V. Kirensky Institute of Physics, Federal Research Center KSC SB RAS, 660036, Krasnoyarsk, Russia

4 Siberian State University of Science and Technology, 660014, Krasnoyarsk, Russia

Published online: 23 November 2019

dynamics (Brownian dynamics) provide a powerful tool for studying characteristics of ions and their interaction with nanoparticles in detail. There are a significant number of papers devoted to the study of EDL of nanoparticles [7–12] on the basis of this method. In particular, the effect of charge discreteness [8, 10] and interaction of ions with their images [12–14] on the EDL structure is studied. It should be noted that mostly dielectric particles are considered in the above papers.

To the best of our knowledge, there is no sufficiently comprehensive model of a metal nanoparticle EDL that would allow to determine its charge, distribution of the potential, and concentration of ions in the vicinity of the nanoparticle taking into account the principal features of electrolyte ions and their interaction with the nanoparticle surface such as the degree of hydration, the size of ions and their mobility, viscosity of the interparticle medium, and existence of specific adsorption as well as the effect of image forces.

The goal of our work is to study the structure of a metallic (silver as an example) nanoparticle EDL depending on the particle size and electrolyte concentration (for NaOH aqueous solution) taking into account all the above factors. The objects of analysis are both nanoparticles themselves and the hydrated ions of the electrolyte medium.

Model

The Brownian dynamics method is employed in this paper as the main tool to study the structure of EDL for various electrolyte concentrations (NaOH) and nanoparticle sizes.

Characterization of hydrated ions

Potential determining ions (PDI) and counterions (CI) interact with each other and with the medium (water) and the nanoparticle during the formation of EDL. Within the framework of the simplified model, they are considered as balls with diameters d_1 and d_2 (see Fig. 1). In particular, for OH^- and Na^+ ions, according to the papers [14–16]; with regard to their hydration shells, we chose the values $d_1 = 0.6$ nm and $d_2 = 0.72$ nm. These ions with the charge q_1 or q_2 ($q_1 = -e$ for PDI and $Q_1 = +e$ for CI, e is an elementary charge) interact electrostatically in a medium with permittivity $\varepsilon = 78$, and collisions between them are absolutely elastic. The existence of hydrate shells limits convergence of OH^- and Na^+ ions to distances that do not allow them to form a stable bond. Indeed, given d_1 and d_2, we obtain the binding energy $e^2/(4\pi\varepsilon_0\varepsilon(d_1/2 + d_2/2)) = 4.47 \cdot 10^{-21}\text{J} \approx k_B T$ at $T = 300$ K.

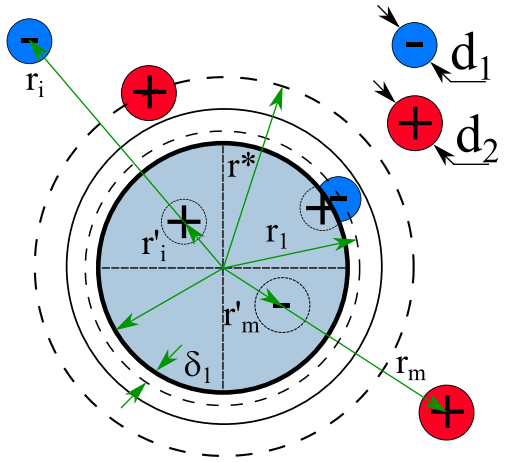

Fig. 1 The scheme of the charge and charge images distribution on the surface of a nanoparticle. Images of ions are shown by dotted lines

Brownian motion of ions

Motion of ions in the medium is considered as the motion of Brownian particles. That is, they are affected by the friction force $\mathbf{F_{fr}}$ determined by the Stokes formula and the random δ—correlated force $\mathbf{F_r}$ having a Gaussian distribution for its projections on the coordinate axes [17]:

$$p(F_{r\,i}) = 2\pi < F_{ri}^2 > \exp\left(-\frac{F_{ri}^2}{2 < F_{ri}^2 >}\right), \quad i = \text{x,y,z} \tag{1}$$

where the root mean square value $< F_{ri}^2 >$ is related to the friction coefficient $\beta = 6\pi\nu r$ by the condition for thermal equilibrium:

$$< F_{ri}^2 >= \beta k_B T/\Delta t, \tag{2}$$

where k_B is the Boltzmann constant, T is the temperature, and Δt is the time step in numerical calculations.

A detailed study of the temperature dependence is beyond the scope of our paper. However, we should note that despite the temperature dependence of the water viscosity and the random force (2) in the temperature range $T = 273 - 373$ K, the characteristics of hydrated ions change negligibly. Temperature variation will affect only the kinetics of the formation of an electric double layer but it will not affect its structure. The particle charge does not depend on the temperature in this range since the interaction energy of PDI with the particle significantly exceeds $k_B T$.

To take into account the motion of ions correctly, the Stokes radius of an ion was also introduced. It was found

from the equality of the friction force and the Coulomb force acting on the ion when moving at a constant speed:

$$6\pi\eta r_s \mathbf{V} = q\mathbf{E}, \quad \mathbf{V} = u\mathbf{E}, \quad r_s = \frac{q}{6\pi\eta u}. \tag{3}$$

Here, u is the ion mobility. In particular, for OH^- (PDI) ions in water, we obtain (at $T = 300$ K) $r_s = 0.047$ nm, and for Na^+ (CI) ions, $r_s = 0.9$ nm, respectively. It is easy to notice a significant difference between the Stokes radii and the hydrated ion radii given above. In particular, for the OH^- ion, this is due to the relay mechanism of charge transfer [18, 19]. This process is considered as charge transfer from the ion to a neighboring water molecule in the absence of ion motion. Thus, the rate of charge transfer increases several times in comparison with the motion of the hydrated ion as a whole.

Ion–nanoparticle interaction

Interaction of ions with a nanoparticle was considered taking into account interaction of each ion with its induced image (Fig. 1). In this case, the Coulomb interaction of ions (before their binding) consists of their interaction with the central charge of the nanoparticle Q_0 and the image charges of all free ions. The force acting on kth ion from the nanoparticle, including images of free ions, can be given by the equation:

$$\begin{aligned}
\mathbf{F}_{np\,k} &= \frac{Q_0 q_k \mathbf{r}_k}{4\pi\varepsilon_0\varepsilon|\mathbf{r}_k|^3} + \frac{1}{4\pi\varepsilon_0\varepsilon}\sum_J \frac{q_k q'_j(\mathbf{r}_k - \mathbf{r}'_j)}{|\mathbf{r}_k - \mathbf{r}'_j|^3}.\\
Q &= Q_0 + \sum_j q'_j, \quad q'_j = -\frac{r}{|\mathbf{r}_j|} q_j\\
\mathbf{r}'_j &= \frac{r^2}{|\mathbf{r}_j|^2}\mathbf{r}_j, \quad |\mathbf{r}'_j| < r < |\mathbf{r}_j|
\end{aligned} \tag{4}$$

Here, Q is the total charge of the nanoparticle equal to the sum of charges of the ions bound with its surface, Q_0 is the charge in the center of the nanoparticle due to the ion image charges, q_j is the charge of the image of the jth ion, and $\mathbf{r}'_j$ is its radius vector.

In addition, an important factor in the interaction of ions with a nanoparticle is the energy of their adsorption to the nanoparticle surface and the characteristic localization distance. As is shown in [20, 21], the average binding energy of an ion^- with the surface of a Ag nanoparticle is $W_{OH} \approx$ 80 kJ/mol or in terms of one ion $W_{OH} \approx 0.83$ eV and due to partial dehydration of the ion it is localized at a distance of $\delta_1 \approx 0.2$ nm from the surface of the nanoparticle. At the same time, binding of Na^+ ions with the nanoparticle is of Coulombic nature and occurs mainly due to interaction with the ion image and OH^-ions bound with the surface. In [14], it is shown that attraction of the image charges of ions is responsible for static and dynamic time-dependent properties of solid polymer electrolytes.

Equations of ion motion and methods of their solution

Thus, we have a set of equations of motion for ions, each having the following form:

$$\begin{aligned}
\frac{d\mathbf{r}_k}{dt} &= \mathbf{V}_k,\\
m_k\frac{d\mathbf{V}_k}{dt} &= \mathbf{F}_{ion,\,k} + \mathbf{F}_{r\,k} + \mathbf{F}_{fr,\,k} + \mathbf{F}_{np,\,k},\\
\mathbf{F}_{ion\,k} &= \frac{1}{4\pi\varepsilon_0\varepsilon}\sum_{J\neq k}\frac{q_k q_j(\mathbf{r}_k - \mathbf{r}_j)}{|\mathbf{r}_k - \mathbf{r}_j|^3},
\end{aligned} \tag{5}$$

Here, m_k is the mass of the kth hydrated ion, $\mathbf{F}_{ion\,k}$ is the Coulomb force acting on the kth ion from all other ions. The motion was simulated in a spherical cell with a nanoparticle placed in its center. The radius of the cell R_0 was chosen for the reasons that the distance from its boundary to the surface of the nanoparticle significantly exceeds the screening radius (the Debye-Hückel radius) λ:

$$\frac{R_0 - r_0}{\lambda} >> 1. \tag{6}$$

Collisions of ions with the domain walls were considered to be perfectly elastic. Since the right-hand side of Eq. 7 is not continuous (due to the presence of a random force), the one-step Runge-Kutta method of the 4th order was used to solve them numerically. The time step (Δt) discretization of the problem is determined by the characteristic correlation time (τ_{cor}) of the ion motion:

$$\begin{aligned}
\tau_{cor} &\sim \min\left(\frac{m_1}{\beta_1}, \frac{m_2}{\beta_2}\right) = \min\left(\frac{m_1 u_1}{e}, \frac{m_2 u_2}{e}\right),\\
\Delta t &< < \tau_{cor}.
\end{aligned} \tag{7}$$

In particular, for the combination of Na^+ and OH^- ions and at temperature $T = 300$ K, we have: $\tau_{cor} \sim 5 \cdot 10^{-14}$ s.

Our simulation yields distribution of the potential and the charge density within EDL. The average local potential was estimated using the Poisson equation and considering that it can significantly fluctuate both in time and space:

$$\Delta\varphi(r) = \frac{1}{\varepsilon_0\varepsilon}\rho.$$

We integrate this equation (applying the condition of spherical symmetry) and obtain an equation for the average value of the potential:

$$\varphi(r) = \int_r^{R_0} \frac{Q_\Sigma(r')}{(r')^2} dr', \quad r \geq r_0. \tag{8}$$

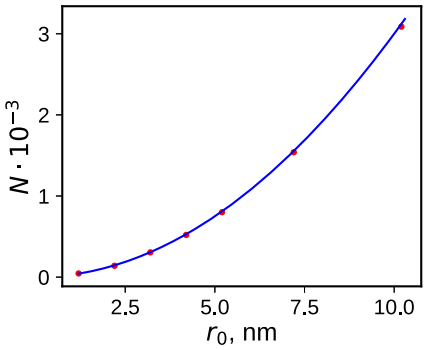

Fig. 2 The number of PDI adsorbed on the particle vs the particle radius

Here, $Q_\Sigma(r)$ is the total charge of nanoparticles and ions, with the centers located within the sphere of radius r ($r_0 \leq r \leq R_0$).

Results

As a result of our simulation, we have found the nanoparticle charge, distribution of potential, and charge density in a steady-state EDL for various concentrations and sizes of nanoparticles at electrolyte temperature 300 K . The binding energy of PDIs with the nanoparticle surface and their mobility significantly exceed the corresponding values for CI. Taking this into account, we believe that the charge of the nanoparticle surface is determined by PDIs rigidly bound with that surface. We can expect them to stay bound to the particle surface until the potential of the sphere of radius r_1 (Fig. 1) reaches $\varphi_{cr} = W_{OH}/e \approx -0.83$ V.

To achieve this condition, even in the absence of an electrolyte, the number of PDIs must exceed $N_{cr} = -4\pi\varepsilon_0\varepsilon r_1\varphi_{cr}/e$. For example, for a particle of radius $r_0 = 1$ nm, we get $N_{cr} \approx 54$. At the same time, our estimates show that a sphere of radius $r_1 = 1.2$ nm for the given sizes of hydrated ions comprises only 45 ions. We can expect that the maximum number of ions located on the surface of a given nanoparticle is limited only by the size of the OH^- ions and the nanoparticle surface. Hereinafter, in the case of large-size particles, we distributed the hydrated ions OH^- randomly (the mean of several realizations was chosen) with the maximum density on the sphere of radius r_1. In this case, the number of ions $N \sim r_1^2$ is shown in Fig. 2. Dependence of the number of ions on the radius of the nanoparticle is well described by the equation $N = 30r_1^2$, where r_1 is given in nanometer. In this case, the layer of PDI has formed a dense inner Stern layer (Fig. 3a). The rest of the electric double layer was formed as a result of the Brownian motion (described by Eq. 5) of the remaining ions. It was expected that with the growth of the particle radius the critical value of the potential would be achieved. Then the mechanism of formation of the internal part of the EDL should change. For example, the distribution of PDIs on the surface of a

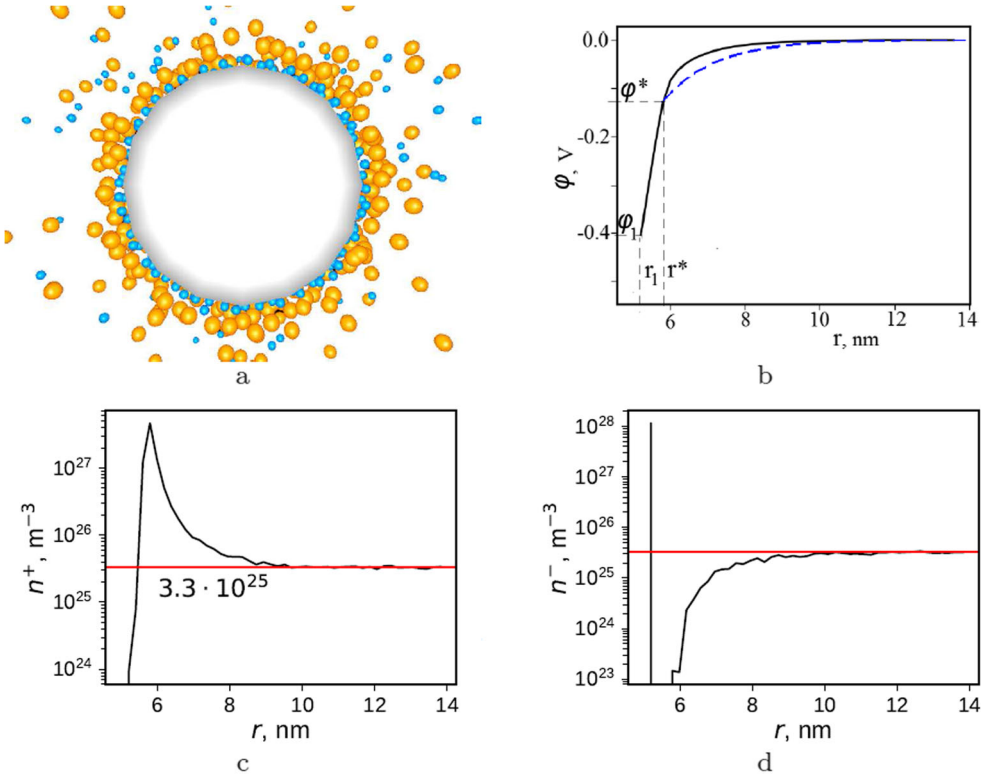

Fig. 3 Distribution of ions on the nanoparticle surface of radius 5 nm. **a** PDI (blue) and CI (yellow). **b** Potential. **c** PDI density. **d** CI density for the average electrolyte concentration 10^{26} m^{-3}

nanoparticle would be more sparse and CIs might be located between them.

Figure 3 shows distribution of ions around a nanoparticle of radius 5 nm for an average electrolyte concentration of $n = 10^{26}$ m^{-3} as well as distribution of the ion potential and concentrations along the cell radius. The same figure shows, for comparison, the theoretical dependence $\varphi(r)$, for the diffuse part ($r \geq r^*$) of the EDL calculated from the following equation [12]:

$$\varphi(r) = \frac{\varphi^* r^*}{4\pi\varepsilon_0\varepsilon r} \exp(-\frac{r - r^*}{\lambda}) \tag{9}$$

Note that the background concentration of electrolyte (at the edge of the computational domain) can be noticeably different from the value averaged over the domain and depends on the particle radius (see Table 1). The Debye-Hückel radius λ was calculated for the background concentration.

We consider a model of an ideal electric double layer including the dense Stern layer and a diffuse part. The inner Stern layer is composed of PDIs whose centers are located on the sphere of radius $r_1 = r_0 + \delta_1$ (see Fig. 1); the outer layer of radius $r^* = r_1 + \delta$ (in our case, the thickness of the Stern layer is $\delta = 0.64$ nm) similarly consists of CIs. Behind this outer layer there is a diffuse part of EDL satisfying the Poisson equation.

For convenience, we introduce surface charge densities for the inner (σ^-) and outer (σ^+) Stern layers.

$$\begin{aligned} Q^- &= -N \cdot e, \\ N &= 30 \cdot r_1^2(nm), \\ \sigma^- &= \frac{Q^-}{4\pi r_1^2} = -\frac{3 \cdot 10^{19} e}{4\pi} \approx 0.382\ (K \cdot m^{-2}), \\ \sigma^+ &= \frac{Q^+}{4\pi (r^*)^2}. \end{aligned} \tag{10}$$

Here, Q^- is the total charge of the inner layer and Q^+ is the charge of the outer layer. The difference in electric potentials between the layers can be defined as follows:

$$\delta\varphi = \varphi(r^*) - \varphi(r_1) = \varphi^* - \varphi_1 = \frac{Q^-}{4\pi (r^*)^2} - \frac{Q^-}{4\pi r_1^2}. \tag{11}$$

Table 1 Background ion concentration n_f in (mol/l)

m^{-3}n, r_0, nm	10^{25}	10^{26}	$5 \cdot 10^{26}$
1	0.013	0.15	0.764
2	0.01	0.11	0.67
3	0.0052	0.052	0.35
4	0.0042	0.035	0.25
5	0.0053	0.55	0.37
7	0.0038	0.037	0.22
10	0.0061	0.055	0.32

Expressing the charge through the surface density, we obtain

$$\delta\varphi = -\frac{\sigma^-}{\varepsilon_0\varepsilon}\left(\frac{r_1}{r^*}\right)(r^* - r_1) = 0.553 \cdot 10^9 \left(\frac{r_1}{r^*}\right)\delta. \tag{12}$$

In Fig. 4, the dependence of the potential jump on r_1 is shown by a black line (4), while the red line (5) shows approximation of the calculated values of $\delta\varphi$, which is well described by a similar equation:

$$\begin{aligned} \delta\varphi' &= -0.553 \cdot 10^9 \left(\frac{r_1}{r'}\right)(r' - r_1), \\ r^* &- r' = 0.045\ nm. \end{aligned} \tag{13}$$

The difference in Eqs. 11 and 12 can be explained by the fact that in reality CIs of the outer Stern layer are not located exactly at the distance δ from the inner layer, but partially penetrate into this layer. That is, in a real situation, the distance $(r^* - r_1)$ between the layers should be slightly shorter. These equations, in particular, show that with increasing nanoparticle radius the potential drop in the Stern layer tends to the finite value:

$$\begin{aligned} \delta\varphi_\infty &= \lim_{R_0 \to \infty} (\delta\varphi) = 0.553 \cdot 10^9 \delta = 0.332\ \text{V}, \\ \delta\varphi'_\infty &= \lim_{R_0 \to \infty} (\delta\varphi') = 0.553 \cdot 10^9 \delta' = 0.307\ \text{V}. \end{aligned} \tag{14}$$

Based on the model of an ideal EDL, we find the potential in the outer part of the Stern layer φ^*.

$$\begin{aligned} \varphi^* &= \frac{Q^-}{4\pi\varepsilon_0\varepsilon r^*} + \frac{Q^+}{4\pi\varepsilon_0\varepsilon r^*} + \int_{r^*}^{R_0} \frac{dq}{4\pi\varepsilon_0\varepsilon r}, \\ dq &= 4\pi r^2 \rho dr \end{aligned} \tag{15}$$

Now we can find the relation between the potential φ^* and the corresponding surface charges. To that end, we estimate the integral on the right side of the equation. Using

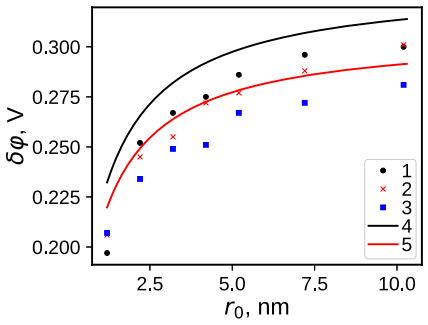

Fig. 4 Dependence of the potential jump $\delta\varphi$ in the Stern layer vs the nanoparticle radius for the specific electrolyte concentrations: 1 – $n = 10^{25}$ m^{-3}, 2 – $n = 10^{26}$ m^{-3}, 3 – $n = 5 \cdot 10^{26}$m^{-3}. 4 and 5 — approximations using Eqs. 12 and 13, respectively

the Poisson equation for the diffuse part of EDL and the corresponding equation for the potential Eq. 9, we find $\rho(r)$:

$$\rho(r) = -\varepsilon_0 \varepsilon \frac{\varphi^* r^*}{\lambda^2 r} \exp\left(-\frac{r - r^*}{\lambda}\right) \tag{16}$$

Substituting $\rho(r)$ into the integral and expressing the charges through their surface densities, we obtain

$$\varphi^* \approx \frac{\lambda}{\varepsilon_0 \varepsilon r^* (r^* + \lambda)} (r_1^2 \sigma^- + r^{*2} \sigma^+) \tag{17}$$

The values of r_1 and r^* increase with growing R_0. However, due to limited σ^- and σ^+ ($|\sigma^+| \leq |\sigma^-|$), the potential in the inner Stern layer (potential of the nanoparticle)

$$\varphi_1 = \varphi^* - \delta\varphi \approx \frac{\lambda}{\varepsilon_0 \varepsilon r^* (r^* + \lambda)} (r_1^2 \sigma^- + r^{*2} \sigma^+) - \\ -\frac{\sigma^-}{\varepsilon_0 \varepsilon} \left(\frac{r_1}{r^*}\right) (r^* - r_1) \tag{18}$$

is also limited.

That is, with an increase in the radius of the nanoparticle, its potential reaches a certain limit value. Moreover, this value grows with the increase of the Debye-Hückel radius λ (or the decrease of electrolyte concentration). This can be clearly seen from the results of numerical calculations presented in Fig. 5. The corresponding approximation based on the following equation is also shown in Fig. 5:

$$\begin{aligned} 1^*- \quad \varphi_1 &= -0.17 - 0.14(r_0 + 0.2)\left(1 - \tfrac{r_0+0.2}{r_0+7.0}\right), \\ 2^*- \quad \varphi_1 &= -0.045 - 0.5(r_0 + 0.2)\left(1 - \tfrac{r_0+0.2}{r_0+1.1}\right), \\ 3^*- \quad \varphi_1 &= 0.016 - 0.54(r_0 + 0.2)\left(1 - \tfrac{r_0+0.2}{r_0+1.0}\right). \end{aligned} \tag{19}$$

Here, r_0 is given in nanometers. From these dependences, we obtain the limits (for $r_0 \to \infty$) for the potential values: 1* — (-1.12 V), 2* — (-0.49 V), 3* — (-0.42 V).

Thus, for significant background electrolyte concentrations ($n_f > 0.1$ mol/l, see the table), we can expect the critical potential φ_{cr} not to be achieved with growing nanoparticle radius. This is possible only at lower concentrations.

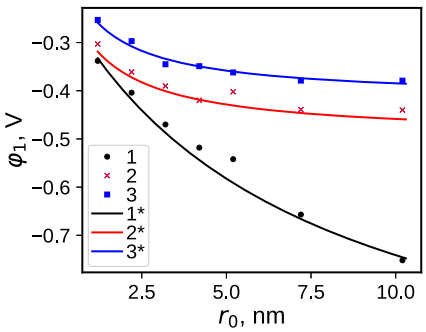

Fig. 5 Dependence of the potential φ_1 of a nanoparticle on its radius for various average electrolyte concentrations: a: $1 - n = 10^{25}$ m^{-3}, $2 - n = 10^{26}$ m^{-3}, $3 - n = 5 \cdot 10^{26}$m^{-3}, 1*, 2*, 3* are approximations using Eq. 19

Conclusion

For the first time, we have presented a detailed model of formation of EDL around metallic nanoparticles in an aqueous electrolyte solution. The model is based on the Brownian dynamics method and covers the formation of not only the diffuse (outer) part of EDL but also the dense Stern layer as well. The studies were carried out for Ag hydrosols as an example with an electrolytic interparticle medium based on NaOH.

The model takes into account the size of hydrated ions, their mobility, and existence of specific adsorption of OH^- ions on the surface of the nanoparticle as well as interaction of ions with their images.

Based on our model, we have determined the charge of a nanoparticle depending on its size as well as its potential φ_1 and the potential jump $\delta\varphi$ in the Stern layer.

It has been shown that the potential φ_1 and the potential jump $\delta\varphi$ tend to finite values as the nanoparticle size increases. Irrespective of the electrolyte concentration $\delta\varphi$ ($r_0 \to \infty$) $\sim$ 0.3 V, and the potential value φ_1 ($r_0 \to \infty$) Eq. 18 drops with decreasing electrolyte concentration.

It has been found that at low electrolyte concentrations ($c \leq 0.1$ mol/l), the total binding energy ($W_{OH} + q_1\varphi_1$) of ions with the particle surface becomes less than $k_B T$, which should result in a change in the charging mode of the particle, formation of the stern layer, and its structure.

As for the distribution of the EDL potential in the diffuse layer, there is a noticeable difference from the results obtained using the generally accepted Debye-Huckel equation, which takes into account screening of the nanoparticle field.

We have identified the principal features of EDL by means of the applied approach. Due to the large charge of a nanoparticle, the effect of interaction of ions with their images is negligible. In addition, the predicted in [22] charge inversion effect associated with reversing the sign of the total charge of both the nanoparticle and the EDLs [23–25] for highly charged nanoparticles has not been detected.

The presented model has made it possible to identify all of the main characteristics of the nanoparticle EDL and their dependence on the particle size and electrolyte concentration.

Funding information The reported research was funded by the Russian Foundation for Basic Research and the government of the Krasnoyarsk territory, Krasnoyarsk Regional Fund of Science, grant No 18-42-243023, the RF Ministry of Education and Science, the State contract with Siberian Federal University for scientific research in 2017–2019.

Compliance with Ethical Standards

Conflict of interests The authors confirm that there are no known conflicts of interest associated with this publication.

References

1. Rao C. N. R., Müller A, Cheetham AK (eds) (2004) The chemistry of nanomaterials. Wiley-VCH Verlag GmbH & Co. KGaA, Weinheim
2. Sonntag H, Strenge K (1970) Koagulation und stabilität disperser Systeme, 173 S., VEB Deutscher Verlag der Wissenschaften, vol 73. Preis: 30.80 MDN, Berlin, p 1971
3. French RH, Parsegian VA, Podgornik R, Rajter RF, Jagota A, Luo J, Asthagiri D, Chaudhury MK, Chiang Y-M, Granick S, Kalinin S, Kardar M, Kjellander R, Langreth DC, Lewis J, Lustig S, Wesolowski D, Wettlaufer JS, Ching W-Y, Finnis M, Houlihan F, von Lilienfeld OA, van Oss CJ, Zemb T (2010) Long range interactions in nanoscale science. Rev Modern Phys 82:1887–1944,6
4. Walker DA, Kowalczyk B, de la Cruz MO, Grzybowski BA (2011) Electrostatics at the nanoscale. Nanoscale 3(4):1316
5. Linse P (2005) Simulation of charged colloids in solution
6. Henderson D, Boda D (2009) Insights from theory and simulation on the electrical double layer. Phys Chem Chem Phys 11:3822, 4
7. Spohr E (1999) Molecular simulation of the electrochemical double layer. Electrochim Acta 44:1697–1705, 1
8. Semashko OV, Brodskaya EN, Us'yarov OG (2005) Molecular dynamics simulation of the electrical double layer of spherical macroion. Colloid J 67:625–630, 9
9. Fahrenberger F, Xu Z, Holm C (2014) Simulation of electric double layers around charged colloids in aqueous solution of variable permittivity. J Chem Phys 141:064902, 8
10. Messina R, Holm C, Kremer K (2001) Effect of colloidal charge discretization in the primitive model. Eur Phys J E 4:363–370, 3
11. Gan Z, Xing X, Xu Z (2012) Effects of image charges, interfacial charge discreteness, and surface roughness on the zeta potential of spherical electric double layers. J Chem Phys 137:169901, 10
12. Torrie GM, Valleau JP, Patey GN (1982) Electrical double layers. II. Monte Carlo and HNC studies of image effects. J Chem Phys 76:4615–4622, 5
13. Emelyanenko KA, Emelyanenko AM, Boinovich L (2015) Image-charge forces in thin interlayers due to surface charges in electrolyte. Phys Rev E 91:032402, 3
14. Izraelashvili JN (2011) Intermolecular and surface forces. Elsevier, Amsterdam
15. Campo MG, Raul Grigera J (2004) Molecular dynamics simulation of OH - in water. Mol Simul 30:537–542, 7
16. Botti A, Bruni F, Imberti S, Ricci MA, Soper AK (2003) Solvation of hydroxyl ions in water. J Chem Phys 119:5001–5004, 9
17. Heermann DW (1990) Computer simulation methods in theoretical physics. Springer, Berlin
18. Tuckerman ME, Chandra A, Marx D (2006) Structure and dynamics of OH - (aq). Account Chem Res 39:151–158, 2
19. Tuckerman ME, Marx D, Parrinello M (2002) The nature and transport mechanism of hydrated hydroxide ions in aqueous solution. Nature 417:925–929, 6
20. Patrito E, Paredes-Olivera P (2003) Adsorption of hydrated hydroxide and hydronium ions on Ag(111). A quantum mechanical investigation. Surf Sci 527:149–162, 3
21. Nechaev IV, Vvedenskii AV (2009) Quantum chemical modeling of hydroxide ion adsorption on group IB metals from aqueous solutions. Protect Met Phys Chem Surf 45:391–397, 7
22. Bunkin NF, Bunkin FV (2003) Screening of strongly charged macroparticles in liquid electrolyte solutions. J Exper Theor Phys 96:730–746, 4
23. Mateescu EM, Jeppesen C, Pincus P (1999) Overcharging of a spherical macroion by an oppositely charged polyelectrolyte. Europhys Lett (EPL) 46:493–498, 5
24. Park SY, Bruinsma RF, Gelbart WM (1999) Spontaneous overcharging of macro-ion complexes. Europhys Lett (EPL) 46:454–460, 5
25. Joanny J (1999) Polyelectrolyte adsorption and charge inversion. Eur Phys J B 9:117–122, 5